

Measuring single molecule conductance with break junctions

Jin He,^a Otto Sankey,^b Myeong Lee,^b Nongjian Tao,^c Xiulan Li^c and Stuart Lindsay^{*abd}

Received 14th June 2005, Accepted 11th July 2005

First published as an Advance Article on the web 15th September 2005

DOI: 10.1039/b508434m

Single-molecule conductance measurements made under potential control provide a critical link between chemical and molecular electronic data. These measurements are made possible by the STM break-junction method introduced recently, but questions remain about its reliability. Here we report the use of a logarithmic current-to-voltage converter to examine a wide range of currents in an STM break junction study of octanedithiol, clearly showing both the gold-quantum wire regime and the single molecule conductance regime. We find two sets of molecular currents that we tentatively ascribe to different bonding geometries of the molecules in the break junction.

Introduction

A key problem in molecular electronics lies in the uncertain nature of the link between electrochemical and optical measurements of charge transfer in solvated molecules (the techniques used by chemists to test their molecules) and charge transfer in a 'dry' molecular electronic device where the surface potential is uncontrolled, and the solvent polarization that stabilizes charging is absent. The STM break-junction is a relatively new method for making measurements of single-molecule conductivity¹ and it lends itself to measurements in conducting solutions² because insulated probes, developed for electrochemical STM, are readily available.³ The ability to measure single molecule conductance in conducting solution now enables direct comparison of electrochemical and molecular electronic properties. Using the technique, we have measured the single molecule conductance of oligoaniline molecules as a function of their oxidation state.⁴ We have also measured changes in the local surface potential caused by the probe to substrate bias as manifested in a negative differential resistance when the applied bias changed the oxidation state of a previously conductive molecule. The effect vanished when the molecule was immersed in toluene, showing how this change of oxidation state was completely inhibited when ions are not present.⁴ In addition, it has recently been demonstrated that non-reversible electrochemistry underlies the negative differential resistance reported at high bias in certain molecular films.^{5,6} The STM break-junction method is a critical tool in such studies, so its reliability, and interpretation of results obtained using it, deserve careful examination. We have already shown elsewhere⁷ that the STM break-junction method appears to be better than the self-assembled single molecule junctions we introduced some years ago⁸ because it is free of artifacts associated with the gold nanoparticles used as contacts for the self-assembled junctions. However, the microscopic nature of the operation of the STM breakjunction is not obvious, because the atomic structure of the junction is not controlled. A recently-introduced technique in which molecules are trapped between fixed electrodes⁹ gives values for the conductance and electronic decay constant (β) of alkanethiols that is much closer to what we

^a Biodesign Institute, Arizona State University, Tempe AZ 85287, USA. E-mail: Stuart.Lindsay@asu.edu

^b Department of Physics and Astronomy, Arizona State University, Tempe AZ 85287, USA

^c Department of Electrical Engineering and Center for Solid State Electronic Research, Arizona State University, Tempe AZ 85287, USA

^d Department of Chemistry and Biochemistry, Arizona State University, Tempe AZ 85287, USA

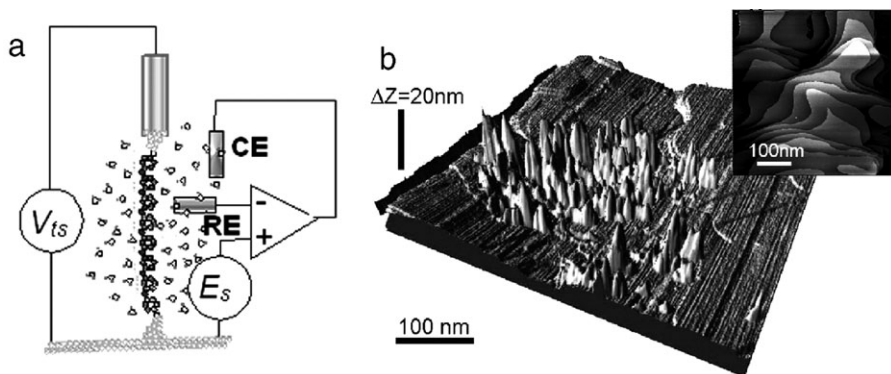


Fig. 1 (a) Showing the apparatus for STM break junction measurements schematically. The STM probe is insulated using techniques developed for electrochemical STM³ enabling potential control of the probe and substrate. (b) The effects of repeated breakjunction formation. The inset (upper right) shows monatomic terraces on a clean gold substrate prior to measurements being made and the 3D image shows how filaments of *ca.* 20 nm height are pulled out of the surface after a series of measurements. This illustrates how the assumption of planar geometry currently used in the simulations may be invalid.

obtained with the nanoparticle method^{8,10} than to the values obtained with the break-junction method.¹ Thus, it appears that the interpretation of STM break junction data is not as clear-cut as first thought, and it is our goal here to describe these newly-discovered complications. We also describe how we select data for analysis in the hope that this will be useful to other laboratories seeking to implement the method. We conclude that the method is reliable to within an order of magnitude or so, but that care is required when comparing different molecules with similar conductances because multiple values can be found for the single molecule conductance. Though simulations do not yet provide a good quantitative explanation of the multiple series of current steps, one explanation is that they arise from different attachments of the molecule to the electrodes.

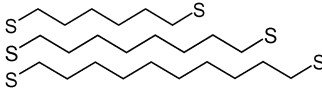
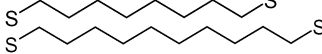
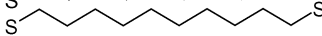
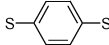
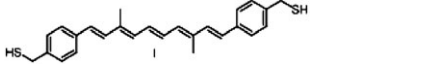
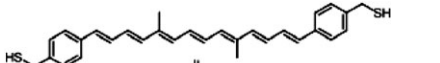
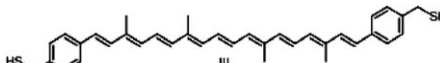
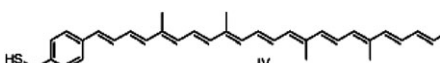
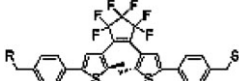
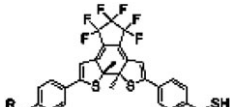
Experimental

The STM break junction

The apparatus is illustrated schematically in Fig. 1a. A gold probe is pushed into a monolayer of molecules that are bis-functionalized with sticky ends (*e.g.*, dithiolates). As the probe is pulled out, the gold necks into a quantum wire showing Landauer steps in conductance.¹¹ Eventually the gold filament breaks, but the gap is often bridged by a molecule. The gold deforms more easily than the molecule¹² so a plot of current *vs.* time shows steps where the conductance remains relatively constant as the gold on either side of the molecule continues to deform as the gap is opened. As first demonstrated for the self-assembled nanojunctions,⁸ a histogram of the gap conductances shows peaks corresponding to 1, 2, 3 *etc.* molecules trapped in the gap. Fig. 1a also illustrates how the measurement can be made with probe and substrate under potential control by insulating the probe almost all the way to its end.³ This arrangement was used for measurements of single molecule conductance under potential control.^{4,6} Fig. 1b shows STM images of the gold surface pre (inset) and post (3D image) a set of measurements, illustrating how gold filaments are drawn out of the surface.

The technique is remarkably simple and a number of molecules have been studied with it in the short time since it was introduced by Xu and Tao.¹ First-principles simulations are available for some of these molecules, and Table 1 shows a comparison of measured and calculated single molecule conductances. With the exception of benzenedithiol (where the disagreement is a factor 50), theory and experiment agree within a factor of about three or better over a range of measured conductances of 2500 : 1. This indicates that, with the possible exception of benzenedithiol, the technique gives reasonably reliable values for single molecule conductance. However, we recently found unexpected extra sets of peaks in the current distributions measured for short oligoanilines (Chen, Nuckolls and Lindsay, unpublished) and this raised questions about the uniqueness of the

Table 1 Comparison of measured and calculated conductances for three alkanedithiols (measurement¹ theory²⁹), benzenedithiol (measurement,³⁰ theory²¹), four carotenoid polyenes¹⁷ and an optically-switched photochromic molecule in two forms¹⁸

Molecule	$G(\text{meas.})/\text{nS}$	$G(\text{theor.})/\text{nS}$	Ratio
	95 ± 6	185	0.51
	19.6 ± 2	25	0.78
	1.6 ± 0.1	3.4	0.47
	833 ± 90	47 000	0.02
	2.6 ± 0.05	7.9	0.33
	0.96 ± 0.07	2.6	0.36
	0.28 ± 0.02	0.88	0.31
	0.11 ± 07	0.3	0.36
	1.9 ± 3	0.8	2.4
	250 ± 50	143	1.74

data obtained from the STM break junction. The observation suggested that perhaps many other sets of peaks would be observed if a greater range of currents were recorded. We therefore decided to return to the simple case of octanedithiol, and to make measurements with a logarithmic current-to-voltage converter so that all possible features in the current-time curve could be revealed in a single experiment.

Data collection with a logarithmic amplifier

We used a logarithmic current to voltage amplifier that was built for our STM by Molecular Imaging (Tempe, AZ). It is based on the diode-feedback circuit described by Durig *et al.*¹³ but uses the BAV199 low-leakage diode (Philips) and a contemporary operational amplifier. The amplifier feedback uses eight diodes (four for each direction of current) across a 1 G Ω resistor, giving rise to a linear response at low currents (<1 nA) a logarithmic response for currents >2 nA. Point by point calibration is required for currents between 1 and 2 nA. This series arrangement of four diodes is important for reducing the contribution of junction capacitance in the feedback loop—the circuit will not work at reasonable speeds with a single diode. The current to voltage conversion was calibrated with a series of resistors (see the figure caption) to yield the calibration curve shown in Fig. 2b. Measurements were made first on clean gold substrates¹⁴ that were hydrogen-flame annealed and submerged in freshly-distilled toluene. The STM tips were formed by cutting a 0.25 mm-diameter Au (Alfa Aesar, 99.999%) wire. They were then immersed in Piranha solution (3 : 1 H₂SO₄ : H₂O₂ (30%) by volume) for 30 s, rinsed with DI water and dried in Ar stream prior to use. **Caution!** Piranha solution is a very strong oxidant and is extremely dangerous to work with; gloves, goggles, and a face shield should be worn. A typical plot of the output of the log amplifier vs. time

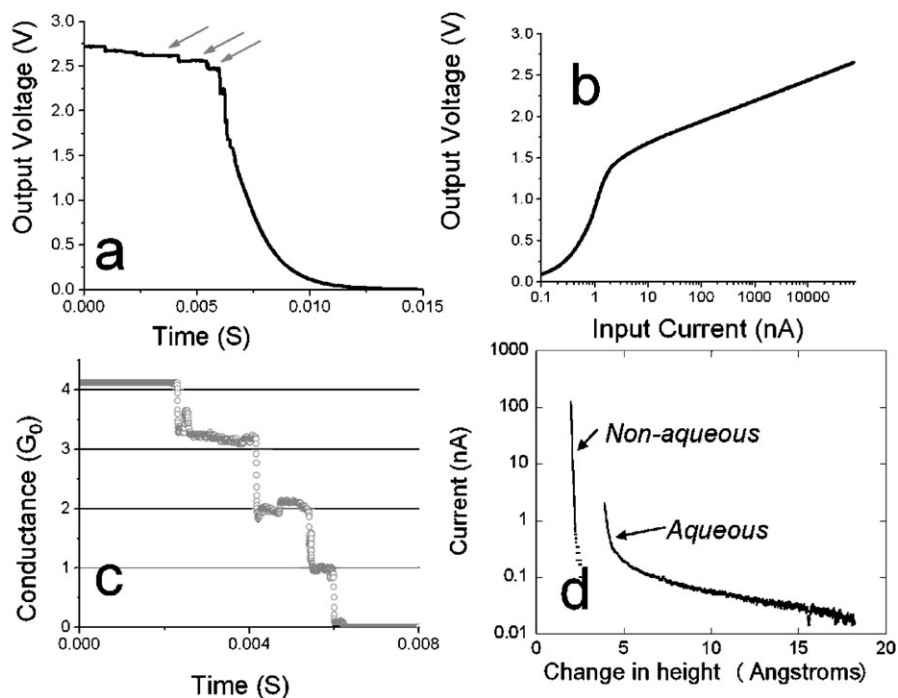


Fig. 2 Current vs. time using a logarithmic amplifier. (a) shows an example of raw output voltage from the log amplifier as a function of time. The structure pointed to by arrows is owing to quantized conductance of the gold wire. (b) Calibration curve for these data. The amplifier has a linear output for small signals with a cross-over to logarithmic behavior near 2 nA, and was calibrated using five different 1% resistors (15 k Ω , 1 M Ω , 10 M Ω , 100 M Ω and 1 G Ω). (c) Linearized data from (a) in the vicinity of the quantum steps showing jumps equal to the Landauer conductance ($e^2/2h$). (d) Examples of control (no molecules) current decay curves after the gold filament is broken for non-aqueous and aqueous environments. A clean surface is signaled by a decay rate of ca. a factor 10 \AA^{-1} in the region immediately following the break.

during a pull is shown in Fig. 2a. Features owing to the quantized conductance of the gold filament are clearly visible, and, when converted to current data using the calibration in Fig. 2b, they reveal the Landauer steps in the conductance, as shown in Fig. 2c.

Cleanliness is of critical importance, and never completely achieved. A measure of the state of the gap is given by the rapidity of the fall-off of current with distance once the wire breaks. This is illustrated in Fig. 2d which shows examples of the tails of the current-time plot for control experiments (no molecules) in toluene and also in aqueous electrolyte (50 mM H₂SO₄). Data obtained in aqueous electrolyte (or in the presence of dissolved molecules) usually decays more slowly at large distances corresponding to the longer electronic decay lengths observed in water¹⁵ but close to point of breakage (where molecules are presumably excluded from the gap) the slope is on the order of a factor ten in current \AA^{-1} , corresponding to the 5 eV workfunction of gold. Such sharp steps are a key indicator of clean data, and we use them as a criterion in selecting data.

Selection of data

The histograms compiled in Fig. 4 were compiled using a selected subset of all the curves. The fraction used varied from 47% to 80% (see the figure caption). In our study of oligoaniline, the fraction used was as small as 20% of the total data set. To retain curves in the final data set, we required that breaks between steps have a slope on the order of a decade \AA^{-1} (arrows on Fig. 3c). The rejected curves either have slopes much larger than this, or are so noisy that slopes cannot be determined. Sharp decay curves with no steps are also rejected because they contribute to the background that peaks at zero current. Noise owing to periodic stray signals can also generate what

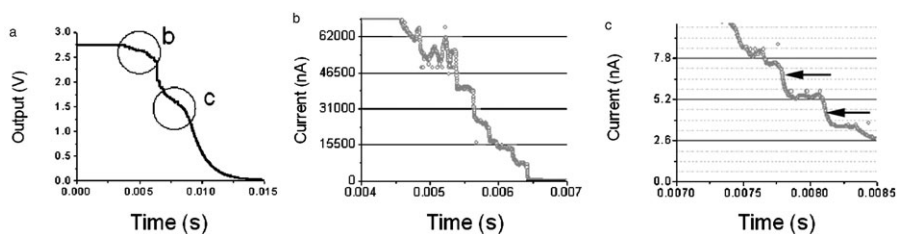


Fig. 3 Data showing both gold-wire quantized conductance and molecular conductance steps at $V = 0.2$ V. (a) Raw output over the entire current range showing distinct gold-wire (labeled 'b') and molecular (labeled 'c') steps. Converted using the calibration shown in Fig. 2b, these data yield current-distance data for the gold-wire steps (b) and the molecular steps (c).

appear to be steps, but these features can be rejected because (a) they occur at equal intervals of time and (b) there are no bias dependent features with this current separation.

Results

1,8-Octanedithiol was purchased from Aldrich and used without further purification. It was dissolved in freshly-distilled toluene to a concentration of 8 mM and introduced into the liquid cell of the microscope immediately after the 'clean' data shown in Fig. 2a were obtained. An example of raw data obtained after the molecules were introduced is shown in Fig. 3a. A new set of features (labeled 'c') has appeared below the Landauer quantum steps (labeled 'b'). Converted to current data, these regions are shown in Fig. 3b (Landauer steps) and 3c (molecular steps). The high

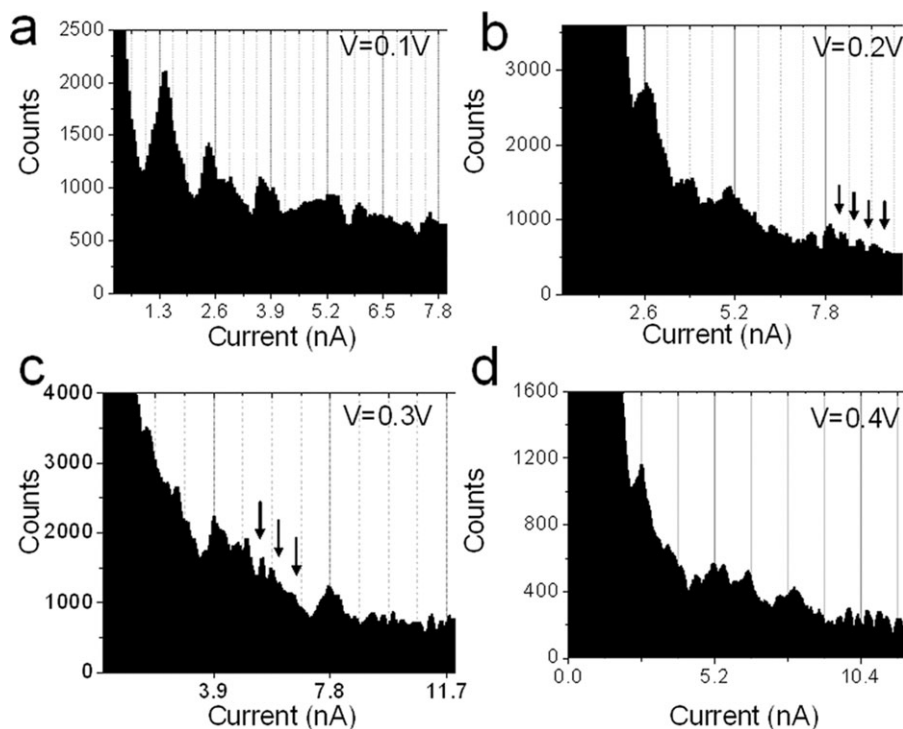


Fig. 4 Current histograms based on data selected as described in the text. Curves are for a tip substrate bias of 0.1 V (a: 132 out of 234 curves used), 0.2 V (b: 340 out of 720 curves used), 0.3 V (c: 357 out of 449 curves used) and 0.4 V (d: 179 out of 249 curves used). In addition to the main series of peaks falling on the gray vertical lines, a secondary series is evident (pointed to by arrows in (c) and (d)).

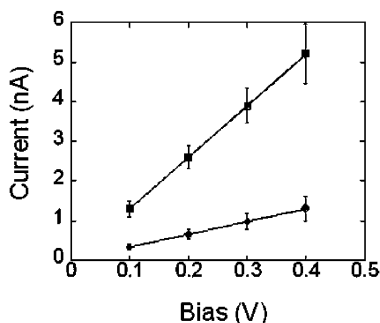


Fig. 5 Current–voltage data derived from histograms like those shown in Fig. 4. The major peak series yields the data shown by the squares, for which $G = 13 \pm 4$ nS. The minor series of peaks yield the data shown by the dots for which $G = 3.25 \pm 1$ nS. Uncertainties are based on an estimate of the relative width of the current peaks in the histogram in order to give an indication of the spread of data. The slope of the current–voltage plots were fitted to a much higher precision.

current region shows steps corresponding to G_0 (with steps at multiples of G_0 washed out as previously reported for gold surfaces with thiol adsorbates¹⁶). Additional steps are now clearly visible in a much lower region of current (see Fig. 3b). Histograms of the current values obtained in the region labeled ‘c’ are shown in Fig. 4. At 0.1 V bias, a clear series of dominant peaks are observed as indicated by the vertical gray bars (which are coincident with the first three well-defined peaks in Fig. 4a). As the bias is increased, new peaks are found at proportionately higher currents as indicated by the vertical gray bars on Fig. 4b, c and d. However, there are also many features in the histogram that do not correspond to the major series in Fig. 4a. Some of these (labeled by arrows) are also clearly periodic with a period that shifts in proportion to the applied bias. Thus there appears to be both a major series of peaks, and a minor series, as well as other less periodic features. Here, as in our other measurements,^{4,17,18} the histogram peaks are seen to broaden considerably as the applied bias is increased. The same effect is seen for the bare gold quantum-wire histograms (data not shown) so this may reflect an increase in gold mobility with increasing electric field as reported by Yasuda and Sakai.¹⁹

Current–voltage data obtained from these two series of current peaks are shown in Fig. 5. The major series would correspond to a single molecule conductance of 13 ± 4 nS, similar to the value of 19 ± 2 nS reported by Xu and Tao.¹ The minor series yields a conductance of 3.25 nS.

Discussion

What is the origin of the extra current features? The value of the electronic decay constant, β , in these alkanethiols is well established as about 1 (carbon atom)⁻¹ added to the chain^{1,20} and this immediately eliminates the possibility that the minor series corresponds to dimers formed by oxidative polymerization of the thiols, because the currents would be a factor more than 2000 times smaller than the monomer currents. Another possibility lies in the detailed nature of the contacts. Theoretical simulations²¹ show that the detailed nature of the bonding (*e.g.*, bonding to top atom sites *vs.* hollow sites) can affect the current by as much as an order of magnitude. Theoretical results for a number of molecules are shown in Table 2 and a factor of 4 is consistent with the magnitude of this effect in other molecules (but see the simulations for alkanedithiols below). Interestingly, the Table shows how the effect is smaller for long molecules (*cf.* the carotenoids) and smaller for the less conducting form of a molecule of a given length (*cf.* the photochromic molecule). This may explain the absence of these additional minor current features in our other published work to date (on an eight-ring oligoaniline⁴ and carotenoids from five to eleven double–single bond pairs¹⁷). It also highlights the difficulty of using this technique on small molecules where this complication appears to be more significant (and, as a further complication, the conductance of dimers may not be negligible for small molecules). These difficulties may account for the significant discrepancy between theory and experiment in the case of benzenedithiol (Table 1).

Table 2 Single molecule conductances for on-top and hollow site bonding calculated for a series of carotenoids¹⁷ (number of double-single bond pairs in parenthesis), benzenedithiol²¹ and a photochromic molecule¹⁸ in both open and closed forms

	G_{top} (nS)	G_{hollow} (nS)	Ratio
Carotene (5db) ¹⁷	7.9	9.7	0.81
Carotene (7db) ¹⁷	2.6	3.5	0.74
Carotene (9db) ¹⁷	0.88	1	0.88
Carotene (11db) ¹⁷	0.3	0.29	1.03
Benzenedithiol ²¹	47 000	5000	9.4
Photochromic (open) ¹⁸	0.84	0.64	1.3
Photochromic (closed) ¹⁸	143	58	2.5

In addition to a series for top–top and hollow–hollow connected molecules, we might expect to observe features that correspond to top–hollow connections. Yet another type of step might consist of parallel combinations of molecules with different connections, for example a top–top connected molecule in parallel with a hollow–hollow connected molecule. Combinations like these might account for some of the extra features observed in the current histograms but better statistics and analysis will be required to clarify this.

Simulations

We have theoretically investigated the effect of binding site on the conductance of alkanedithiol molecules. Two sites were chosen; the hollow site (the thiol is above three Au atoms on a Au (111) surface), and the on-top site where the thiol directly bonds to a single Au atom in a Au surface (111) plane. The distance between the hollow site and S was 1.90 Å, and the distance between S and the on-top-Au was 2.42 Å.^{22,23} The bond angle of S with the Au site and C on the chain was 119°. The theoretical method used was Green's function scattering theory for the Landauer transmission analysis.²¹ The electronic structure method used was a local-orbital density functional method with pseudopotentials.^{24–26}

We find the somewhat surprising result that the relative ordering of the conductance at the two sites depends on the length of the alkane chain. Table 3 lists the conductances for the two sites as a function of number of carbons N in the chain. The hollow site gives a larger conductance at short length, while the on-top site gives the larger conductance at large length. There is a crossover length where the two sites give an equal conductance, although in this specific case it happens for the relatively short $N = 4$ chain. For the specific chain of length eight carbon atoms (octanedithiol), there is only a 12% difference between the two conductances ($G_{\text{top}}/G_{\text{hollow}} = 1.12$). The calculated value of G_{top} is within a factor of two of the higher current data, and the calculated value of G_{hollow} is within a factor of eight. Thus, while the effect is present, these simulations fail to capture its full extent. One important factor may be the use of a planar Au(111) model for the contact; a glance at Fig. 1b shows how inappropriate this is. More realistic models of the contact geometry will require simulations of much greater complexity.

Nonetheless, these simulations point to some unexpected features. The crossover occurs because of a competition involving two effects. The first is the coupling of the molecule with the two Au contacts. We'll call these contributions G_c . The factor G_c includes the density of states of the metal and interaction couplings between the molecule and metal and at first glance one might expect that the ratio of the conductances would be the ratio of two values of G_c for the two geometries. The second effect is the difference in propagation through the molecule, which we will write simply as $e^{-\beta N}$. The decay parameter β is a property of the molecule. However, it depends on the relative alignment of molecular states with the Au Fermi level, $\beta(E_F)$. The Fermi level lineup with the molecular states depends on the bonding site of the molecule with the Au. The level shift is quite substantial; the Fermi level moves from away from near mid-gap toward the HOMO by about 0.5 eV in the on-top bonding geometry. In this specific molecule, such a large shift does not produce huge effects as might normally be expected since the band-gap of the molecule (in DFT) is about

Table 3 Calculated values of conductance for a series on alkanedithiols attached to on-top and hollow sites on Au(111). The present simulation produced a result about 5% different from the earlier simulation cited in Table 1

N	G_{top}/nS	$G_{\text{hollow}}/\text{nS}$	Ratio
4	1260	1290	0.98
6	208	174	1.20
8	26.4	23.6	1.12
10	4.29	3.15	1.36
12	0.67	0.43	1.56

10 eV.²⁷ The data shown in Table 2 yield $\beta_{\text{top}} = 0.95$ (carbon atom)⁻¹ and $\beta_{\text{hollow}} = 1$ (carbon atom)⁻¹ and $G_c = 71 \mu\text{S}$ for the hollow site and $56 \mu\text{S}$ for the on-top site (from $G = G_c e^{-\beta N}$).

Comparison of results obtained with the various methods

Haiss *et al.*⁹ use a technique in which the probe is brought very close to the surface and the current recorded as a function of time in the presence of dithiolated molecules. Jumps are observed in the current-time trace and when the frequency of these jumps is recorded as a function of their magnitude, peaks are found, presumably corresponding to 1, 2, 3 *etc.* molecules in the gap. The magnitudes of the currents are much closer to what was reported using the gold nanoparticle contacts^{8,10} than to the results first reported by Xu and Tao using the break-junction method¹ (although Haiss *et al.* did report the observation of much higher current steps as well⁹). Furthermore, Haiss *et al.* found a value for β of 0.52 methylene⁻¹, close to the value reported using nanoparticle contacts¹⁰ (0.57) and in disagreement with the result of *ca.* 1.0 reported by Xu and Tao,¹ found in simulations²⁷ and deduced from many other experimental methods (see references in Cui *et al.*¹⁰).

The agreement between the results of the break-junction method and theory is striking. Xu and Tao¹ reported that the low-bias single molecule conductance agreed well with simulations but this remarkable degree of agreement is better illustrated by plotting the theoretical results²⁷ together with the data¹ on the same plot (Fig. 6a). Of course, the smaller current series reported here would not be in such excellent agreement, but this agreement suggests that the major current series corresponds closely to what was modeled in the simulations.

The results obtained with a nanoparticle contact⁸ are plotted in Fig. 6b as the thicker solid line. The data obtained by Haiss *et al.*⁹ are shown by the squares. The two sets of data agree well at low bias, and the observation of a small value for β for both sets suggests a common origin. We

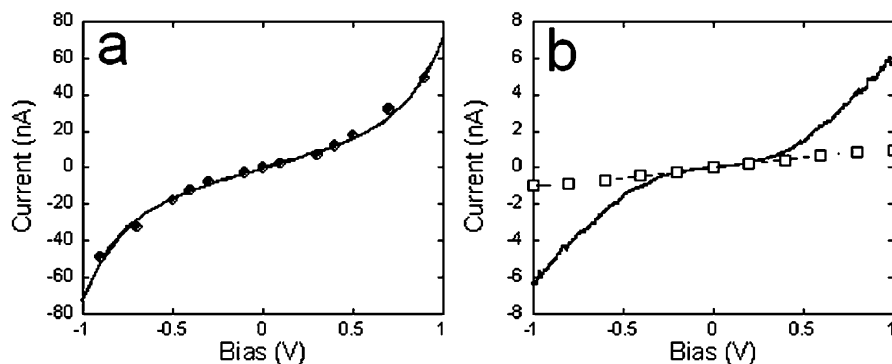


Fig. 6 (a) Dots show data for octanedithiol as reported by Xu and Tao.¹ The solid line shows the results of a first-principles simulation with *no* adjustable parameters.²⁷ Data and simulation are shown on the same scale with no adjustment or scaling of any sort. (b) The line shows average current–voltage data (*ca.* 1000 molecules) for octanedithiol on Au with a 1.5 nm diameter Au nanoparticle contact.⁷ The squares are data for octanedithiol obtained by trapping the molecule in a fixed gap.⁹

explained our data qualitatively as the result of the electronic structure of the nanoparticle combined with charging of the nanoparticle.⁷ We also showed that smaller nanoparticles extended the voltage range over which the current–voltage characteristic was linear.⁷ It is therefore possible that the data of Haiss *et al.* correspond to molecules terminated in a gold atom (or small cluster) at one end. If this were the case, then the larger current jumps (*ca.* $\times 10$) reported by them may correspond to direct connections to the electrodes without isolated atoms or clusters. Jumps between states where the molecule is either attached directly to the electrode, or parted from it, but still terminated by one or more gold atoms have been proposed as an explanation of so-called stochastic switching.²⁸ We note further that such charging is thermally-activated and thus might give rise to significant temperature dependence of the current.

Conclusions

We have shown here that the STM break junction provides data for single molecule conductance that appear to be reliable to within about an order of magnitude. By using a logarithmic current to voltage converter, we have shown that, in the case of octanedithiol, molecular conductance steps and gold-wire quantum conductance steps each occupy a distinct, well separated region of currents. There appear to be no spurious signals outside these regions, though the nature of the gold quantum wire steps is modified by the presence of a molecular adlayer. In addition to a major series of conductance peaks separated by 13 ± 4 nS, a second series was observed corresponding to 3.25 ± 1 nS and tentatively attributed to different atomic arrangements of the contacts, though simulations do not account for the full extent of the effect. Other features are observed in the histograms, but their assignment requires further study. The correct assignment of peaks is essential when comparing data from molecules of similar composition but slightly different length, as done when determining the electronic decay length. Multiple sets of current peaks were not a problem in our study of carotenoids¹⁷ but they have complicated our analysis of data obtained from oligoanilines of various lengths (unpublished data).

Acknowledgements

We thank Bingqian Xu for useful discussions. Rich Nichols and David Schiffrin provided useful comments on our first draft of this ms. This work was supported by a NIRT grant of the NSF (ECS 01101175).

References

- 1 B. Xu and N. J. Tao, *Science*, 2003, **301**, 1221.
- 2 B. Xu, P. M. Zhang, X. L. Li and N. J. Tao, *Nano Lett.*, 2004, **4**, 1105.
- 3 L. A. Nagahara, T. Thundat and S. M. Lindsay, *Rev. Sci. Instrum.*, 1989, **60**, 3128.
- 4 F. Chen, J. He, C. Nuckolls, T. Roberts, J. Klare and S. M. Lindsay, *Nano Lett.*, 2005, **5**, 503.
- 5 J. He and S. Lindsay, *J. Am. Chem. Soc.*, 2005, submitted.
- 6 X. Xiao, L. Nagahara, A. Rawlett and N. J. Tao, *J. Am. Chem. Soc.*, 2005, in press.
- 7 J. Tomfohr, G. Ramachandran, O. F. Sankey and S. M. Lindsay, in *Introducing Molecular Electronics*, ed. G. Fagas and K. Richter, Springer, Berlin, 2005.
- 8 X. D. Cui, A. Primak, X. Zarate, J. Tomfohr, O. F. Sankey, A. L. Moore, T. A. Moore, D. Gust and S. M. Lindsay, *Science*, 2001, **294**, 571.
- 9 W. Haiss, R. J. Nichols, H. van Zalinge, S. J. Higgins, D. Bethell and D. J. Schiffrin, *Phys. Chem. Chem. Phys.*, 2004, **6**, 4330.
- 10 X. D. Cui, A. Primak, X. Zarate, J. Tomfohr, O. F. Sankey, A. L. Moore, T. A. Moore, D. Gust, L. A. Nagahara and S. M. Lindsay, *J. Phys. Chem. B*, 2002, **106**, 8609.
- 11 C. Z. Li, X. E. He and N. J. Tao, *Appl. Phys. Lett.*, 2000, **77**, 3995.
- 12 B. Xu, X. Xiao and N. J. Tao, *J. Am. Chem. Soc.*, 2003, **125**, 16164.
- 13 U. Durig, L. Novotny and B. Michel, *Rev. Sci. Instrum.*, 1997, **68**, 3814.
- 14 J. A. DeRose, T. Thundat, L. A. Nagahara and S. M. Lindsay, *Surf. Sci.*, 1991, **256**, 102.
- 15 A. Vaught, T. W. Jing and S. M. Lindsay, *Chem. Phys. Lett.*, 1995, **236**, 306.
- 16 C. Z. Li, H. Sha and N. J. Tao, *Phys. Rev. B*, 1998, **58**, 6775–6778.
- 17 J. He, F. Chen, J. Li, O. F. Sankey, Y. Terazono, C. Herrero, D. Gust, T. A. Moore, A. L. Moore and S. M. Lindsay, *J. Am. Chem. Soc.*, 2005, **127**, 1384.
- 18 J. He, F. Chen, P. A. Liddell, J. Andréasson, S. D. Straight, D. Gust, T. A. Moore, A. L. Moore, J. Li, O. F. Sankey and S. M. Lindsay, *Nanotechnology*, 2005, **16**, 695.

-
- 19 H. Yasuda and A. Sakai, 1997, **56**, 1069–1072.
 - 20 X. D. Cui, X. Zarate, J. Tomfohr, A. Primak, A. L. Moore, T. A. Moore, D. Gust, G. Harris, O. F. Sankey and S. M. Lindsay, *Nanotechnology*, 2002, **13**, 5.
 - 21 J. K. Tomfohr and O. F. Sankey, *J. Chem. Phys.*, 2004, **120**, 1542.
 - 22 J. Tomfohr, *Electrontunneling transport theory for molecules*, PhD Thesis, Arizona State University, Tempe, AZ, 2002.
 - 23 H. Kondoh, M. Iwasaki, T. Shimada, K. Amemiya, T. Yokoyama, T. Ohta, T. Shimomura and S. Kono, *Phys. Rev. Lett.*, 2003, **90**, 066102.
 - 24 J. P. Lewis, K. R. Glaesemann, P. Voth, J. Fritsch, A. A. Demkov, J. Ortega and O. F. Sankey, *Phys. Rev. B*, 2001, **64**, 195103.
 - 25 A. A. Demkov, J. Ortega, O. F. Sankey and M. P. Grumbach, *Phys. Rev. B*, 1995, **52**, 1618.
 - 26 O. F. Sankey and D. J. Niklewski, *Phys. Rev. B*, 1989, **40**, 3979.
 - 27 J. Tomfohr and O. F. Sankey, *Phys. Rev. B*, 2002, **65**, 245105.
 - 28 G. K. Ramachandran, T. J. Hopson, A. M. Rawlett, L. A. Nagahara, A. Primak and S. M. Lindsay, *Science*, 2003, **300**, 1413.
 - 29 J. Tomfohr and O. F. Sankey, *Phys. Status Solidi B*, 2002, **233**, 59.
 - 30 X. Xiao, B. Q. Xu and N. J. Tao, *Nano Lett.*, 2004, **4**, 267.